

Support Curvature and Conformational Freedom Control Chemical Reactivity of Immobilized Species

Tino Zdobinsky, Pradipta Sankar Maiti, and Rafal Klajn*

Department of Organic Chemistry, Weizmann Institute of Science, Rehovot 76100, Israel

S Supporting Information

ABSTRACT: We show that bimolecular reactions between species confined to the surfaces of nanoparticles can be manipulated by the nature of the linker, as well as by the curvature of the underlying particles.

For many decades, enzymes have impressed scientists with the elegance with which they control chemical reactions. With their abilities to activate, preorganize, and increase local concentrations of substrate molecules, they have inspired chemists to design novel systems in which improved reactivities emerge.¹ In one example, Liu and co-workers induced dramatic acceleration of bimolecular reactions between substrates by preorganizing them on nucleic acid templates.² Other templates that were used to bring molecules together include self-assembled cages³ as well as surfaces of inorganic materials.⁴ However, increasing effective molarity alone is not enough to induce efficient bimolecular reactions; as we demonstrate in this study, lack of sufficient conformational freedom can drastically suppress chemical reactivity despite greatly increased local concentrations of the reactive moieties. Further, we show that reactivity of surface-confined species can be controlled by tailoring the flexibility of the linker chains, as well as by manipulating the curvature of the underlying nanoparticle (NP) surface.

Ethynylanthracenes^{5–7} are attractive substrates for studying the effect of molecular confinement on chemical reactivity. In the absence of the C≡C triple bond, anthracenes undergo the well-known^{8–11} [4+4] dimerization when exposed to long-wave ($\lambda \sim 365$ nm) UV irradiation. The presence of the triple bond at the 9-position, however, alters the reaction pathway so as to induce a selective [4+2] Diels–Alder dimerization^{12–14} under the same reaction conditions. Recently, Weiss and co-workers have demonstrated that upon binding to Au(111) surfaces, thiol **1** dimerizes in the [4+4] fashion despite the presence of the triple bond;^{14,15} that is, the “normal” behavior of unsubstituted anthracenes is restored. These researchers argued that the planar surface acts as a template favoring molecular arrangements ideal for the [4+4], but not for the [4+2], cycloaddition. Inspired by these findings and motivated by the many advantages of NPs over planar surfaces,¹⁶ we synthesized thiolated 9-ethynylanthracenes **1–3** and investigated their photoreactivities within self-assembled monolayers on metallic nanospheres.

Our initial experiments were based on 2.5 nm gold NPs functionalized with the previously reported^{14,17–19} 9-(4-mercaptophenylethynyl)anthracene (Figure 1b). These and

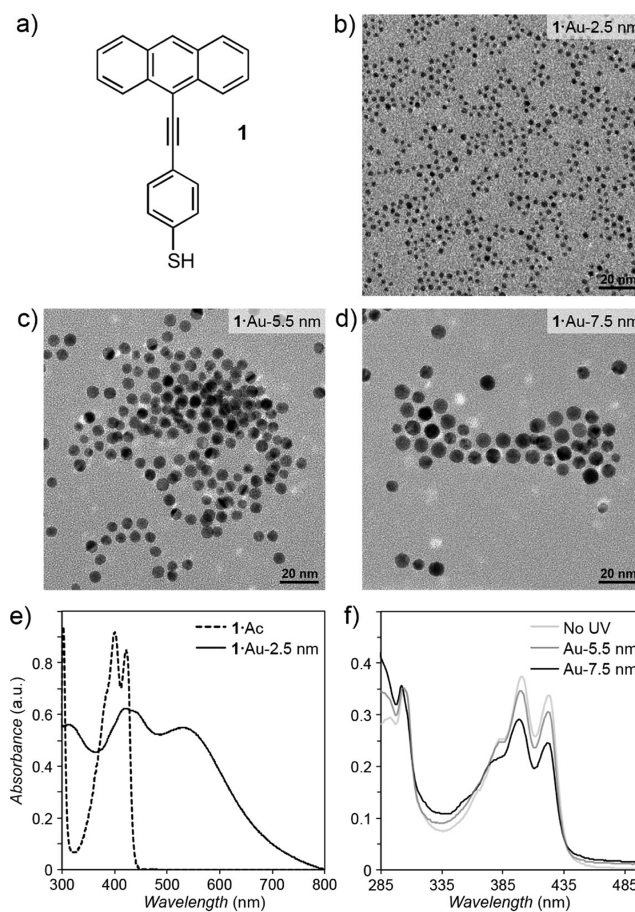


Figure 1. (a) Structural formula of 9-(4-mercaptophenylethynyl)anthracene **1**. (b–d) TEM images of **1**-functionalized 2.5 nm, 5.5 and 7.5 nm Au NPs, respectively. (e) UV–vis spectra of small-molecule **1** (in the form of a thioacetate; pure **1** is highly unstable), and the NPs shown in (b). The broad band at ~ 550 nm is due to surface plasmon resonance. (f) UV–vis spectra of **1** released from 5.5 nm (dark gray) and 7.5 nm (black) Au NPs preirradiated under the same conditions ($t = 21$ h). Also shown (light gray) is a spectrum of **1** released from nonirradiated 2.5 nm NPs. The spectra were normalized with respect to the same initial concentration of **1**.

other NPs investigated in this study were prepared via ligand exchange reaction using preformed, dodecylamine (DDA)-capped NPs²⁰ and excess of free thiol, followed by

Received: November 13, 2013

Published: December 9, 2013

precipitation, thorough washing to remove any nonadsorbed thiols, and finally redispersion in pure toluene. As shown in Figure 1e, binding to Au NPs alters the optical properties of **1**, red-shifting and significantly broadening the characteristic absorption band at ~ 400 nm. We then exposed the samples to $\lambda \sim 365$ nm UV light at ~ 0.7 mW/cm², an intensity sufficient to induce both [4+2] and [4+4] dimerization reactions^{14,21} while not affecting the stability of thiolate monolayers²² on metallic NPs under investigation. Both dimerization reactions can conveniently be followed by UV-vis spectroscopy: the Diels–Alder reaction results in the blue-shift of the anthracene absorption bands,¹² whereas the [4+4] dimerization manifests itself by a practically complete disappearance of absorption above ~ 300 nm.²³ While unadsorbed **1-Ac** in solution underwent facile [4+2] Diels–Alder dimerization upon UV irradiation (compare Figures S1 and S2 in the Supporting Information), no changes in the UV-vis spectra of NP-anchored **1** were observed even after continuous exposure of the samples to 24 h of UV light under the same illumination conditions ($I \sim 0.7$ mW/cm²). This result suggests that the large curvature of the 2.5 nm NPs prohibits two anthracene moieties from assuming orientation required for dimerization to occur. Interestingly, our observations are in agreement with the recent findings that the [4+4] reaction on rough Au surfaces is greatly suppressed as compared to the atomically flat ones.²¹

To confirm the important role of the substrate curvature, we also prepared and functionalized larger, ~ 5.5 and ~ 7.5 nm Au NPs (**1-Au-5.5** nm and **1-Au-7.5** nm in Figure 1c,d).²⁴ Unfortunately, we found that once precipitated (during the purification procedure), these larger particles were insoluble in toluene or other solvents, presumably due to poor solvation of the π – π -stacked ligands. However, the on-surface reactivity could still be investigated; we UV-irradiated the stable solutions of these NPs in the presence of free **1** and, following selective removal and washing of NPs, released the surface-bound molecules using an optimized cyanide etching protocol²⁵ (see Supporting Information, page S9).²⁶ UV-vis spectra of thus released **1** are shown in Figure 1f, whereby the decreased absorption in the anthracene region is an indication of the [4+4] dimerization; by comparing peak intensities, we conclude that the yield of the reaction is $\sim 9\%$ and $\sim 26\%$ on 5.5 and 7.5 nm NPs, respectively.²⁷

In addition to decreasing NP curvature, the [4+4] dimerization might be encouraged by providing the anthracene groups with extra conformational freedom, for example, by incorporating alkylene bridges. To test this hypothesis, we synthesized 9-ethynylacetylenes **2** and **3** (equipped with additional $-(\text{CH}_2)_2-$ and $-(\text{CH}_2)_5-$ linkers, respectively; Figure 2a). Again, gold particles decorated with these ligands could not be solubilized: as soon as **2** and **3** were added to solutions of differently sized DDA-protected Au NPs, rapid precipitation commenced. However, we found, somewhat surprisingly, that palladium NPs with diameters nearly identical to those of the smallest Au NPs were readily soluble in toluene when protected with **1**, **2**, **3**, or any combinations thereof (cf. Figure 2b for monodisperse 2.6 nm Pd NPs coated with **1**). Moreover, the absence of surface plasmon resonance in palladium made it possible to decouple the optical response of the ligands from that of Pd, and to quantify the coverage of the particles with **1**–**3** (Figure 2c–f and page S10 of the Supporting Information). The results are rather unexpected: while both **2** and **3** formed densely packed monolayers on Pd

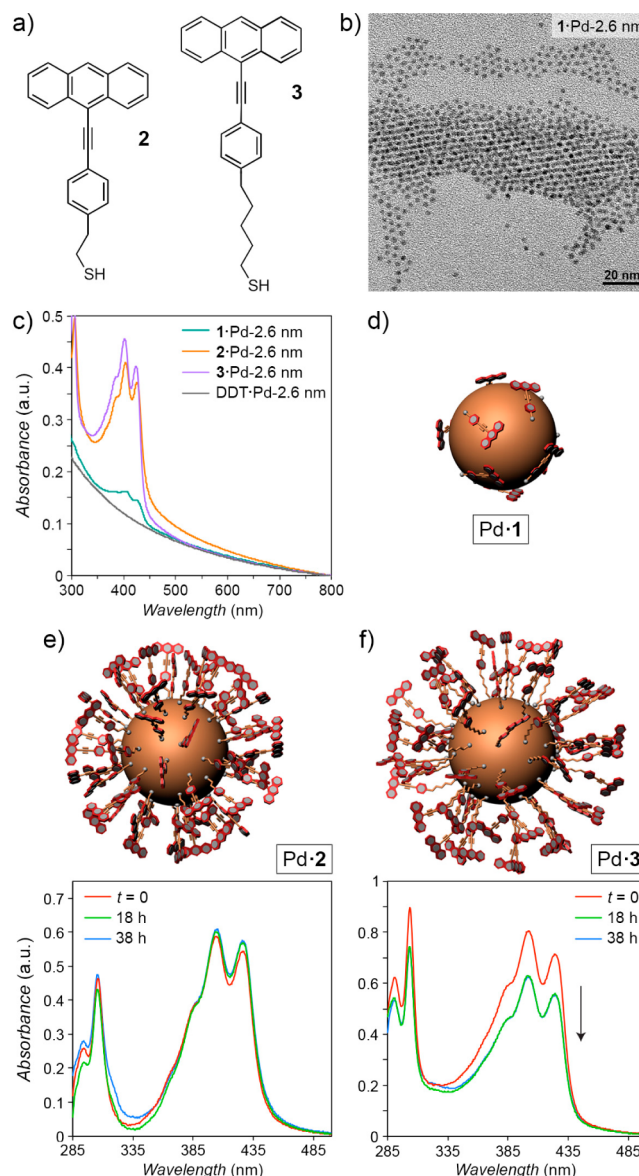


Figure 2. (a) Structural formulas of ethynylanthracenes **2** and **3**. (b) TEM image of **1**-functionalized 2.6 nm Pd NPs. (c) UV-vis spectra of Pd NPs functionalized with **1**, **2**, **3**, and dodecanethiol (DDT). (d) Schematic representation of a Pd NP covered with 9 molecules of ligand **1**. The particle surface is likely cofunctionalized with residual DDA molecules. (e) Schematic representation of a Pd NP covered with 58 molecules of ligand **2** and (below) no changes in the UV-vis spectra of these particles upon UV irradiation.

(57.9 and 57.8 molecules per NP; corresponding to ~ 0.364 nm² per molecule; compare to ~ 0.214 nm² occupied by a single alkyl thiolate ligand within densely packed monolayers on planar gold), as little as 8.6 molecules of **1** could be accommodated on a single Pd particle, corresponding to an average surface area of ~ 2.51 nm² taken by each molecule. On the basis of these numbers, it is reasonable to propose two different binding modes of these thiols to Pd NPs: **2** and **3** are oriented normal to the particle surface, whereas **1** maximizes contact with the surface,^{28,29} as schematically presented in Figure 2d–f. We hypothesize that this transition is due to lateral van der Waals interactions between alkylene chains in **2** and **3**, since no such interactions are possible in **1**.

Among all Pd NPs subjected to UV irradiation, only 3-Pd-2.6 nm showed changes in the UV-vis spectra (Figure 2f, bottom), where the intensity of the anthracene bands decreased by ~21% after 18 h of UV light. Exposure to an additional 20 h of UV did not result in any further decrease of the signal, indicating that the number of anthracene units able to assume orientation necessary for the dimerization to take place does not increase with time (at least within our time scales), e.g., as a result of ligand migration.

Finally, we considered the possibility of an on-nanoparticle Diels-Alder reaction between the C≡C triple bond dienophile of a shorter ligand (**1** or **2**), and the anthracene diene of a longer ligand (**2** or **3**) (Figure 3e). Toward this end, we

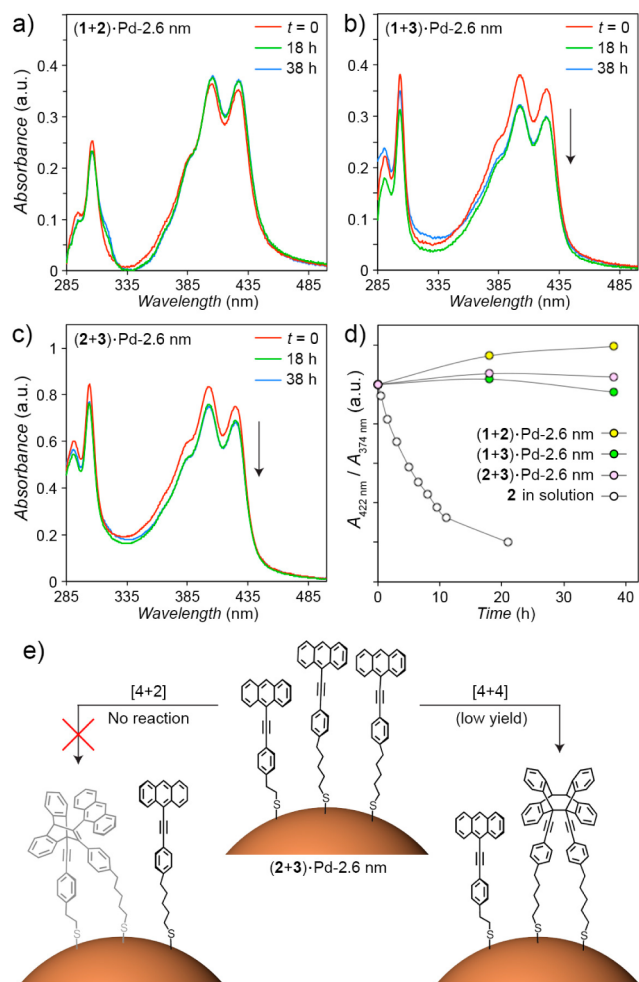


Figure 3. (a) Changes in the UV-vis spectra of NPs protected with the different mixed monolayers upon UV irradiation. (d) Following the progress of the Diels-Alder reaction in solution and on NPs. (e) Schematic representation of the behavior of mixed monolayers.

prepared 2.6 nm Pd NPs functionalized with mixed monolayers of **1+2** (Figure 3a), **1+3** (Figure 3b), and **2+3** (Figure 3c). Notably, the 1:1 ratio of thiols used for surface modification was similar to that on the resulting NPs,³⁰ although we were unable to accurately determine the composition of the mixtures on NPs due to the different absorption coefficients of **1**, **2** and **3** (Figures S5–S10 in the Supporting Information). The progress of the Diels-Alder reaction can be followed using UV-vis spectroscopy by comparing the absorbance at $\lambda = 422$ nm (high for the substrate (anthracene coupled to the C–C triple bond);

low for the product (isolated anthracene)) to that at $\lambda = 374$ nm (low for the substrate; high for the product; compare with Figure S3 in the Supporting Information). As Figure 3d shows, no indication of the [4+2] cycloaddition between NP-bound ligands was found, even in (2+3)-Pd, where both ligands are expected to be oriented perpendicular to the surface as schematically presented in Figure 3e. On the other hand, both types of NPs functionalized with mixed monolayers containing **3** showed a decrease of the overall anthracene absorbance, suggesting that the most flexible **3** can dimerize in the [4+4] fashion even in the presence of additional, unreactive ligands **1** and **2** on the same NPs (based on the UV-vis spectra, we estimate that the conversion was ~16% and ~9% for (1+3)-Pd and (2+3)-Pd, respectively).

In sum, we investigated chemical reactivity of arylolefinylanthracenes on the surfaces of metallic nanoparticles. We found that (i) although no [4+4] dimerization is observed on 2.5 nm NPs functionalized with the rigid **1**, the reaction can be induced by decreasing the NP curvature; (ii) the mode of binding of **1–3** to Pd NPs is critically dependent on the presence of the alkylene linker; (iii) the [4+4] reaction can also be induced by introducing a flexible (and appropriately long) linker between the anthracene moiety and the particle surface; and (iv) the Diels-Alder reaction was blocked on the surfaces of NPs, highlighting the importance of substrate preorganization in bimolecular reactions. We believe these results contribute to our understanding of chemical reactivity within confined environments, and are of interest in the context of the development of new sensing and catalytic systems.

■ ASSOCIATED CONTENT

Supporting Information

Synthesis and characterization of **1–3**; preparation, functionalization and characterization of Au and Pd nanoparticles. This material is available free of charge via the Internet at <http://pubs.acs.org>.

■ AUTHOR INFORMATION

Corresponding Author

rafal.klajn@weizmann.ac.il

Funding

This work was supported by the Israel Science Foundation (Grant No. 1463/11).

Notes

The authors declare no competing financial interest.

■ REFERENCES

- (1) Meeuwissen, J.; Reek, J. N. H. *Nat. Chem.* **2010**, *2*, 615–621.
- (2) Li, X. Y.; Liu, D. R. *Angew. Chem., Int. Ed.* **2004**, *43*, 4848–4870.
- (3) Yoshizawa, M.; Klosterman, J. K.; Fujita, M. *Angew. Chem., Int. Ed.* **2009**, *48*, 3418–3438.
- (4) Fruchtel, J. S.; Jung, B. *Angew. Chem., Int. Ed.* **1996**, *35*, 17–42.
- (5) Godinez, C. E.; Zepeda, G.; Garcia-Garibay, M. A. *J. Am. Chem. Soc.* **2002**, *124*, 4701–4707.
- (6) Goldsmith, R. H.; Vura-Weis, J.; Scott, A. M.; Borkar, S.; Sen, A.; Ratner, M. A.; Wasielewski, M. R. *J. Am. Chem. Soc.* **2008**, *130*, 7659–7669.
- (7) Fudickar, W.; Linker, T. *J. Am. Chem. Soc.* **2012**, *134*, 15071–15082.
- (8) Bouas-Laurent, H.; Castellan, A.; Desvergne, J. P.; Lapouyade, R. *Chem. Soc. Rev.* **2000**, *29*, 43–55.
- (9) Grimme, S.; Diedrich, C.; Korth, M. *Angew. Chem., Int. Ed.* **2006**, *45*, 625–629.
- (10) Fox, M. A.; Wooten, M. D. *Langmuir* **1997**, *13*, 7099–7105.

(11) Bhola, R.; Payamyar, P.; Murray, D. J.; Kumar, B.; Teator, A. J.; Schmidt, M. U.; Hammer, S. M.; Saha, A.; Sakamoto, J.; Schlüter, A. D.; King, B. T. *J. Am. Chem. Soc.* **2013**, *135*, 14134–14141.

(12) Becker, H. D.; Andersson, K. *J. Photochem.* **1984**, *26*, 75–77.

(13) Yuasa, J.; Ogawa, T.; Kawai, T. *Chem. Commun.* **2010**, *46*, 3693–3695.

(14) Kim, M.; Hohman, J. N.; Cao, Y.; Houk, K. N.; Ma, H.; Jen, A. K. Y.; Weiss, P. S. *Science* **2011**, *331*, 1312–1315.

(15) Zheng, Y. B.; Pathem, B. K.; Hohman, J. N.; Thomas, J. C.; Kim, M.; Weiss, P. S. *Adv. Mater.* **2013**, *25*, 302–312.

(16) It is possible to probe a large number of surface-bound molecules in a single experiment; the molecules can readily be investigated using techniques such as NMR and UV–vis spectroscopy; one can etch the NP templates to release the organic molecules; the effect of curvature (i.e., differently sized nanospheres) can be investigated; etc.

(17) Zareie, M. H.; Ma, H.; Reed, B. W.; Jen, A. K. Y.; Sarikaya, M. *Nano Lett.* **2003**, *3*, 139–142.

(18) Dou, R. F.; Ma, X. C.; Xi, L.; Yip, H. L.; Wong, K. Y.; Lau, W. M.; Jia, J. F.; Xue, Q. K.; Yang, W. S.; Ma, H.; Jen, A. K. Y. *Langmuir* **2006**, *22*, 3049–3056.

(19) Fang, L.; Park, J. Y.; Ma, H.; Jen, A. K. Y.; Salmeron, M. *Langmuir* **2007**, *23*, 11522–11525.

(20) Jana, N. R.; Peng, X. G. *J. Am. Chem. Soc.* **2003**, *125*, 14280–14281.

(21) Zheng, Y. B.; Payton, J. L.; Song, T.-B.; Pathem, B. K.; Zhao, Y.; Ma, H.; Yang, Y.; Jensen, L.; Jen, A. K. Y.; Weiss, P. S. *Nano Lett.* **2012**, *12*, 5362–5368.

(22) Witt, D.; Klajn, R.; Barski, P.; Grzybowski, B. A. *Curr. Org. Chem.* **2004**, *8*, 1763–1797.

(23) Wu, D. Y.; Zhang, L. P.; Wu, L. Z.; Wang, B. J.; Tung, C. H. *Tetrahedron Lett.* **2002**, *43*, 1281–1283.

(24) Chovnik, O.; Balgley, R.; Goldman, J. R.; Klajn, R. *J. Am. Chem. Soc.* **2012**, *134*, 19564–19567.

(25) Zhu, T.; Vasilev, K.; Kreiter, M.; Mittler, S.; Knoll, W. *Langmuir* **2003**, *19*, 9518–9525.

(26) As a control experiment, we subjected free **1** (protected as a thioacetate) to etching conditions and verified that it did not affect the UV–vis spectra.

(27) Notably, we find no indication (cf. Figure 3) of the Diels–Alder reaction between the NP-bound **1** and the same molecules moving around freely in solution.

(28) Likely by coordinating with the C≡C triple bond to the Pd surface.

(29) Schramm, A.; Stroh, C.; Dossel, K.; Lukas, M.; Fischer, M.; Schramm, F.; Fuhr, O.; von Lohneysen, H.; Mayor, M. *Eur. J. Org. Chem.* **2013**, 70–79.

(30) We found that the total numbers of anthracene moieties per NP were in the following ranges: (1+2)·Pd, 29.3–31.7 ligands/NP; (1+3)·Pd, 23.1–28.6 ligands/NP; (2+3)·Pd, 48.2–55.5 ligands/NP.